

1 **Title**

2 **Replenishing Age-Related Decline of IRAK-M Expression in Retinal Pigment Epithelium**
3 **Attenuates Outer Retinal Degeneration**

4

5 **Authors**

6 Jian Liu^{1*}, David A. Copland¹, Alison J. Clare¹, Mathias Gorski², Burt T. Richards³, Louis Scott¹,
7 Sofia Theodoropoulou¹, Ursula Greferath⁴, Katherine Cox¹, Oliver H. Bell¹, Kepeng Ou¹, Jenna
8 Le Brun Powell⁵, Jiahui Wu¹, Luis Martinez Robles⁶, Yingxin Li⁵, Lindsay B. Nicholson^{1,6}, Peter
9 J. Coffey⁷, Erica L. Fletcher⁴, Robyn Guymer⁸, Monte J. Radeke⁹, Iris M. Heid², Gregory S.
10 Hageman³, Ying Kai Chan^{1,10}, Andrew D. Dick^{1,6,7,11}

11

12 **Affiliations**

13 ¹Academic Unit of Ophthalmology, Bristol Medical School, University of Bristol, Bristol, United
14 Kingdom.

15 ²Department of Genetic Epidemiology, University of Regensburg, Regensburg, Germany.

16 ³Sharon Eccles Steele Center for Translational Medicine, John A. Moran Eye Center, University
17 of Utah School of Medicine, Salt Lake City, Utah, United States.

18 ⁴Department of Anatomy and Physiology, University of Melbourne, Victoria, Australia.

19 ⁵Translational Health Sciences, Bristol Medical School, University of Bristol, Bristol, United
20 Kingdom.

21 ⁶School of Cellular and Molecular Medicine, University of Bristol, Bristol, United Kingdom.

22 ⁷Institute of Ophthalmology, University College London, London, United Kingdom.

23 ⁸Centre for Eye Research Australia, Royal Victorian Eye and Ear Hospital, University of
24 Melbourne, Melbourne, Australia.

25 ⁹Neuroscience Research Institute, University of California, Santa Barbara, California, United
26 States.

27 ¹⁰Wyss Institute for Biologically Inspired Engineering, Harvard University, Boston,
28 Massachusetts, United States.

29 ¹¹National Institute for Health Research Biomedical Research Centre, Moorfields Eye Hospital,
30 London, United Kingdom.

31

32 *Correspondence should be addressed to Dr. Jian Liu (jian.liu@bristol.ac.uk).

33

34

35 **One Sentence Summary**

36 IRAK-M is a protective molecule and promising therapeutic target for macular degeneration

37

38

39

40 Abstract

41 Unchecked, chronic inflammation is a constitutive component of age-related diseases, including
42 age-related macular degeneration (AMD). Here we identified interleukin-1 receptor-associated
43 kinase (IRAK)-M as a key immunoregulator in retinal pigment epithelium (RPE) that declines
44 with age. Rare genetic variants of IRAK-M increased the likelihood of AMD. IRAK-M expression
45 in RPE declined with age or oxidative stress and was further reduced in AMD. IRAK-M-deficient
46 mice exhibited increased incidence of outer retinal degeneration at earlier ages, which was further
47 exacerbated by oxidative stressors. The absence of IRAK-M disrupted RPE cell homeostasis,
48 including compromised mitochondrial function, cellular senescence, and aberrant cytokine
49 production. IRAK-M overexpression protected RPE cells against oxidative or immune stressors.
50 Subretinal delivery of AAV-expressing IRAK-M rescued light-induced outer retinal degeneration
51 in wild-type mice and attenuated age-related spontaneous retinal degeneration in IRAK-M-
52 deficient mice. Our data support that replenishment of IRAK-M expression may redress
53 dysregulated pro-inflammatory processes in AMD, thereby treating degeneration.

54

55

56

57

58

59

60

61

62

63

64

65

66

67

68

69

70

71

72

73

74

75

76

77

78

79

80

81

82 **Main Text**

83

84 **INTRODUCTION**

85 Cell-autonomous responses such as metabolic regulation, autophagy and immune-mediated
86 inflammation initiated by noxious stress (environmental factors) are active processes that help to
87 maintain homeostasis (1). However, loss of immune regulation and persistent inflammation beget
88 divergent or excessive immune responses, leading to detrimental acute or chronic tissue damage.
89 Such chronic inflammation is accentuated by age (inflammageing) and implicated in progression
90 of many age-related degenerative disorders (2).

91 The retinal pigment epithelium (RPE) is essential for maintenance of outer retinal function and
92 ocular immune privilege. Dysfunction of the RPE leads to photoreceptor (PR) loss and gradual
93 loss of the central visual acuity, as observed in age-related macular degeneration (AMD) (3-5).
94 AMD is a progressive, multifactorial disease that is a leading cause of irreversible severe vision
95 loss in the elderly. Alongside ageing, the interplay of oxidative stress and chronic inflammation,
96 resulting from genotype-predisposed susceptibility and environmental stressors, is a significant
97 driver of AMD. Multiple genome-wide association studies have identified risk loci for late and/or
98 early AMD, including, but not exclusively, genes in the complement pathway and *ARMS2/HTRA1*
99 alleles (6, 7). Specifically, rare coding variants in regulatory genes of complement such as *CFH*
100 and *CFI* have been associated with AMD risk. This knowledge has led to developing therapeutics,
101 including complement inhibitors and gene therapies for augmenting regulators of complement
102 pathway (8, 9). Notwithstanding there remain a number of pathological pathways implicated in
103 the pathogenesis of AMD, including oxidative stress and innate immune responses (10, 11). In
104 mice, for example, a high fat diet is required to illuminate pathology on the background of
105 complement gene mutation (12). Therefore, elucidating factors central to the diverse pathologies
106 in AMD is critical, irrespective of genetic risk.

107 Multiple inflammatory pathways are associated with AMD progression, including activation of
108 the complement cascade and NLRP3 inflammasome, production of cytokines and chemokines
109 (e.g., IL-1 β , IL-6, IL-8, IL-12, MCP-1, and TNF- α), and low levels of infiltrating cells to the outer
110 retina, such as dendritic cells and macrophages, as well as immune-activated microglia and RPE
111 (13-17). Emerging evidence also indicates the association of Toll-like receptors (TLRs),
112 particularly TLR2, 3 and 4, in the risk of development of AMD (18-20). The Myddosome is an
113 oligomeric complex consisting of an adaptor protein MyD88 and IL-1R-associated kinase (IRAK)
114 family proteins, and required for transmission of both TLR and inflammasome-IL-1R axis-
115 mediated signals (16). Conversely, Myddosome signalling also promotes inflammasome
116 activation (21). Although an overactivation of the Myddosome has been observed in the RPE from
117 patients with geographic atrophy (GA, late stage of atrophic AMD) (16), important questions
118 remain to be determined such as whether the overactivation has a pivotal role in AMD progression
119 and which component(s) of the Myddosome complex lead to the dysregulation of TLR/IL-1R pro-
120 inflammatory signaling cascades.

121 Highlighting a central role in the pathophysiology of the retina, the RPE exhibits the highest
122 number of differentially expressed genes (DEGs) overlapping with the genes associated with
123 ageing and age-related retinal diseases and is highly susceptible to the perturbation of ageing and

124 inflammatory stressors (22). When the disturbance in RPE intracellular processes, such as
125 autophagy, phagolysosome, mitochondrial metabolism, protein trafficking and senescence, is
126 compounded by oxidative stress, inflammation is elaborated by inflammasome activation and IL-
127 1 β /IL-18 release (17, 23, 24). Associated with tissue and organ damage in clinical scenarios such
128 as neurodegeneration, cancer and pulmonary diseases, the magnitude of oxidative stress-induced
129 inflammation is largely determined by various TLRs and balanced by counteracting mechanisms
130 regulated by inhibitors including IRAK-M (gene symbol *IRAK3*) (25, 26). Acting as a
131 pseudokinase, IRAK-M downregulates the pro-inflammatory cascade by impeding the uncoupling
132 of phospho-IRAK1/4 from the Myddosome for TGF- β -activated kinase 1 (TAK1)-dependent NF-
133 κ B activation, or by forming an IRAK-M/MyD88 complex that stimulates the second wave of NF-
134 κ B activation to induce inhibitory modulators (27, 28).

135 IRAK-M is expressed in organs including the liver, heart, brain, spleen, kidney, and thymus (29).
136 Downregulation of IRAK-M signalling is associated with exaggerated oxidative stress and
137 systemic inflammation in metabolic disorders such as insulin resistance and obesity. Reduced
138 IRAK-M expression in monocytes and adipose tissues of obese subjects leads to elevated
139 mitochondrial stress, systemic inflammation, and metabolic syndrome (30). Multiple mutations in
140 *IRAK3* have been associated with early-onset chronic asthma in humans (31).

141 Following our finding of IRAK-M protein expression in the RPE, a study of IRAK-M in retinal
142 ageing and degeneration was undertaken. We determined the role of IRAK-M in the development
143 of AMD by evaluating genetic variants and their association with AMD risk, evaluating expression
144 of IRAK-M in patient samples and mouse models, and also evaluating changes in retinal function
145 in transgenic mice lacking IRAK-M. Overall, the expression of IRAK-M within human and mouse
146 retinas showed an RPE-specific decline with ageing and was associated with the induction of
147 oxidative stress. RNA-Seq data mining and histology studies divulged a lower IRAK-M
148 expression level in AMD eyes compared to age-matched controls. *Irak3*^{-/-} mice developed earlier
149 pathological changes in the retina and RPE with age than wild-type mice, which was accentuated
150 by oxidative stressors. Finally, by overexpressing IRAK-M, we demonstrate a protective role of
151 IRAK-M maintaining RPE cell function and homeostasis, thereby curbing retina degeneration in
152 mouse models.

153

154 RESULTS

155 Rare protein-altering variants of *IRAK3* are associated with increased risk of late AMD

156 In view of the observation of Myddosome activation in AMD (16), we asked whether changes in
157 the Myddosome components contribute to disease risk and pathogenic pathways. Analysis of rare
158 variants that alter peptide sequences (non-synonymous), truncate proteins (premature stop), or
159 affect RNA splicing (splice site) can help to identify causal mechanisms – particularly when
160 multiple associated variants reside in the same gene (32). Based upon the genetic data from the
161 International AMD Genomics Consortium (IAMDGC) that contains 16,144 late AMD cases
162 versus 17,832 age-matched controls (6), we found no genetic association between rare variants of
163 *MYD88* and late AMD ($P = 0.95$). We then examined the cumulative effect of rare protein-altering
164 variants for all IRAK family kinases (*IRAK1-4*). Among these 4 closely related candidate genes,
165 our analysis highlighted a statistically significant late AMD risk-increasing signal for *IRAK3* ($P =$

166 0.012) (Table 1). Table S1 lists the variants in the *IRAK3* gene region, including 18 polymorphic
167 variants that were detected in both AMD cases and controls and used in the gene burden test. As
168 a comparator for *IRAK3*, rare variants of *IL33* that encodes a Th2-oriented cytokine linked to
169 retinal pathophysiology (33-35) were not associated with late AMD ($P = 0.18$).
170

171 **Table 1. Rare protein-altering variants of *IRAK3* is associated with increasing risk of late AMD by**
172 **IAMDGC genomic analysis.**

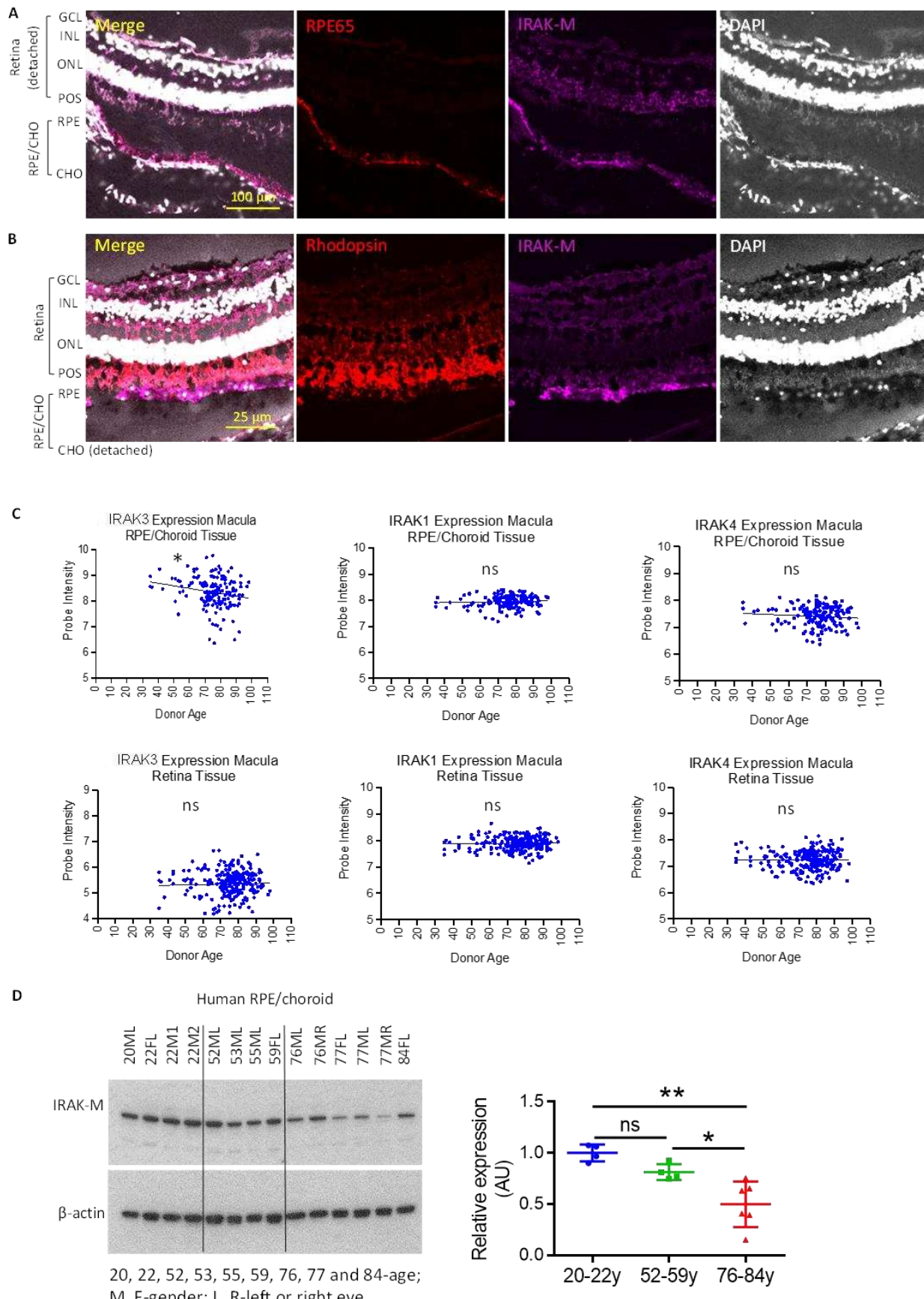
Gene Symbol	CHROM	Start	End	N Markers	Increasing/decreasing risk for AMD	P value
<i>IRAK3</i>	12	66,582,994	66,648,402	18	Increasing risk	0.012
<i>IRAK1</i>	X	153,278,500	153,284,192	2	Increasing risk	0.35
<i>IRAK2</i>	3	10,219,555	10,280,654	12	Increasing risk	0.91
<i>IRAK4</i>	12	44,172,041	44,177,510	3	Decreasing risk	0.22

173 The cumulative effect of rare protein-altering variants in the 16,144 late AMD cases versus 17,832 controls
174 of four IRAK genes in the IAMDGC data was examined using gene burden test.
175
176

177 **IRAK-M expression in RPE is reduced with age and to a greater extent in AMD patients**

178 IRAK-M expression was originally reported to be expressed solely by monocytes and
179 macrophages (36). As we observed *IRAK3*'s association with late AMD risk, we explored IRAK-
180 M expression in the retina by performing immunohistochemistry on frozen human retinal sections
181 from a young donor eye (20y old, no recorded eye diseases). The data showed an abundant IRAK-
182 M distribution at the RPE layer of the retinal sections, which were co-stained with anti-RPE65
183 (Fig. 1A) and anti-rhodopsin (Fig. 1B), respectively. Weaker immunopositivity of IRAK-M was
184 found within other retinal layers, including GCL (ganglion cell layer), IPL (inner plexiform layer),
185 OPL (outer plexiform layer), ONL (outer nuclear layer), POS (PR outer segment) and choroid
186 (Fig. 1A and B). Negative controls with primary antibody omitted did not show any signal. An
187 independent immunohistochemistry experiment also demonstrated IRAK-M expression by human
188 RPE in the RPE/choroidal sections from a 73y-old male donor (without recorded eye diseases;
189 Fig. S1A and B). Similar to human expression, IRAK-M was expressed in the mouse RPE (Fig.
190 S1C-E) and a human RPE cell line ARPE-19 (Fig. S1F). These findings are consistent with our
191 previously reported detection of IRAK-M transcript in a murine RPE cell line *in vitro* (23). We
192 also observed strong immunopositivity of IRAK-M in both inner (non-pigmented) and outer
193 (pigmented) ciliary epithelium of human eyes (Fig. S1G and H), emphasizing a potential
194 regulatory role in barrier cells.

Fig. 1



196 **Fig. 1. IRAK-M is expressed in RPE and its expression level is reduced with age and in AMD. (A&B)**

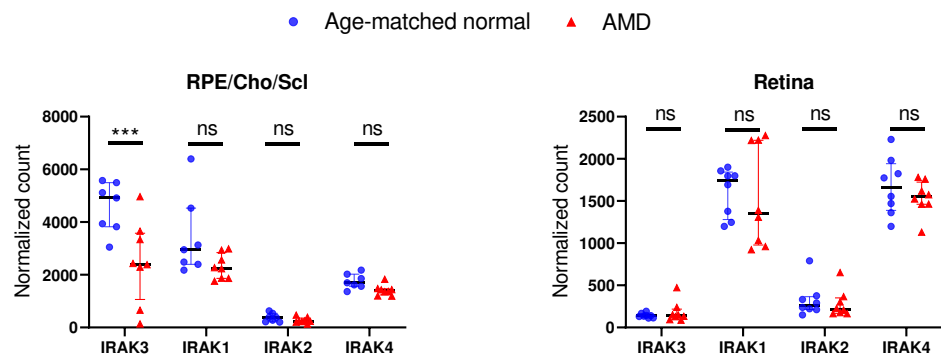
197 Confocal images of human retinal sections from a 20-year-old donor (without recorded ocular disease) demonstrate IRAK-M immunopositivity at the RPE layer (anti-RPE65 stain). DAPI and anti-Rhodopsin were used to stain nuclei and POS, respectively. (C) Affymetrix chip-based transcriptome analyses show an age-related reduction in the expression level of *IRAK3* mRNA in macular RPE/choroid tissues, but not in the retina. Neither *IRAK1* nor *IRAK4* mRNA level is changed with age in RPE/choroid or retina. (D) Western blot and densitometry quantification show reduced levels of IRAK-M protein expression in aged human RPE/choroidal lysates. The IRAK-M levels were normalized to β -actin (n=4-6). *P < 0.05; **P < 0.01; ns, nonsignificant. Comparison by simple linear regression (C) or one-way ANOVA (D).

205
206 We next determined whether the expression level of IRAK-M altered during ageing, the essential
207 pre-requisite for developing AMD. Microarray of human eye samples (without recorded eye
208 diseases) identified an age-dependent decrease in *IRAK3* transcript levels in the macular (Fig. 1C)
209 and extramacular (Fig. S2) RPE/choroid. There was no change in expression in the retina (Fig. 1C
210 and Fig. S2). Neither *IRAK1* nor *IRAK4* altered with age in RPE/choroid or retina (Fig. 1C and
211 Fig. S2). Further analyses of IRAK-M protein expression in human RPE/choroid lysates across a
212 range of ages revealed significant reduction in elderly samples (76-84y) compared to young (20-
213 22y) and middle-aged (52-59y) samples (Fig 1D). In parallel with reduced IRAK-M protein
214 expression, increased levels of phospho-IRAK4 and NF- κ B p65 were detected (Fig. S3A),
215 supporting activation of inflammatory signaling pathways. CFH and C3 protein expression did not
216 change with age (Fig. S3A). As with human samples, RPE isolated from aged mice (19-24m;
217 correlating to a human age of approximately 75 years (31)) had lower IRAK-M protein levels
218 compared with younger mice (2-5m, Fig. S3B). The expression of IRAK-M protein in mouse
219 retinal CD11b+ cells (MACS-isolated-microglia and perivascular macrophages) was also reduced
220 with age (Fig. S3C).

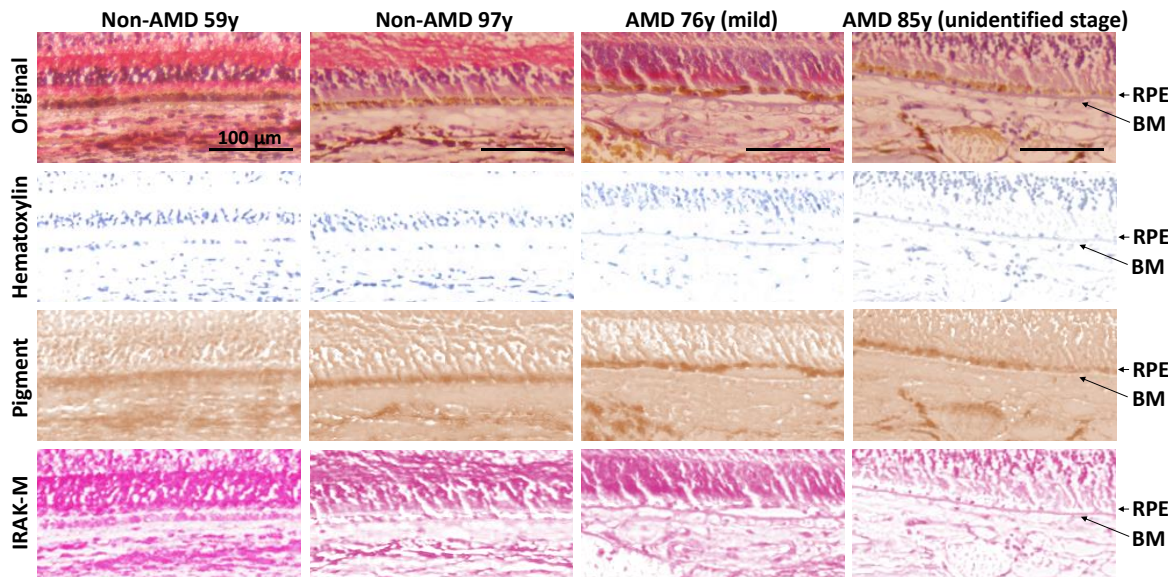
221 We further sought to ascertain whether IRAK-M expression was compromised in AMD, as
222 compared to age-matched controls. We analyzed a published RNA-Seq dataset (GSE99248),
223 which included PORT-normalized counts for both sense and antisense transcripts (37). When
224 assessing all *IRAK* family genes, we found that only the level of *IRAK3* mRNA in
225 RPE/choroid/sclera, and not in the retina, was significantly lower in AMD than age-matched
226 controls (Fig. 2A). *IRAK1*, *IRAK2* and *IRAK4* expression, as well as antisense RNAs specific to
227 any *IRAK*, were unchanged between AMD and controls (Fig. 2A). From the same dataset, we also
228 examined the expression of other known genes for negative regulation of TLR/IL-
229 1R/MyD88/IRAK1/4 signalling (Fig. S4), including *PIN1* (peptidylprolyl cis/trans isomerase,
230 NIMA-interacting 1, which inhibits TLR transcription factor IRF3), *IL1RN* (IL-1R antagonist),
231 *SOCS1* (suppressor of cytokine signaling 1, which induces MAL ubiquitination required for
232 MyD88 activation), *TOLLIP* (Toll-interacting protein, which binds to IRAK1 to induce
233 translocation of TLRs to endosome for degradation), *FADD* (Fas-associated death domain, which
234 interacts with IRAK1/MyD88 to attenuate the signaling), and *PTPN6* (Tyrosine-protein
235 phosphatase non-receptor type 6, which inhibits SYK activation and blocks MyD88
236 phosphorylation). None of these genes showed any significant difference between AMD and
237 controls.

Fig. 2

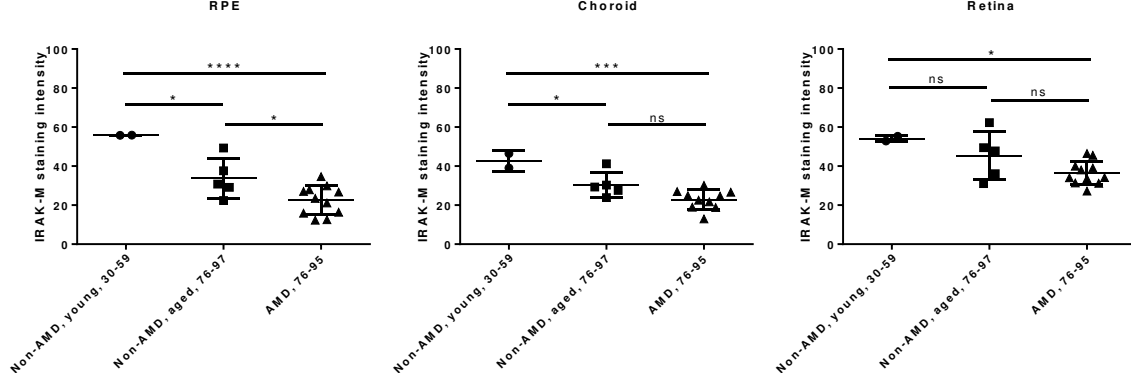
A



B



C



238

239 **Fig. 2. IRAK-M expression level in RPE is reduced in AMD.** (A) PORT-normalized gene counts from
240 RNA-Seq data (GSE99248) show decreased *IRAK3* mRNA expression in RPE/Choroid/Sclera of AMD
241 donors versus age-matched normal controls. *IRAK1*, *IRAK2* and *IRAK4* mRNA levels in
242 RPE/Choroid/Sclera have no difference. Nor mRNA levels of any *IRAKs* in retina show difference (n=7-
243 8). (B) Magnification of boxed regions of representative IHC images (Fig. S5) of human retinal sections
244 from two non-AMD (59-year and 97-year old, respectively), a mild AMD (76-year old), and an unidentified
245 stage AMD donors (85-year old) were color-deconvoluted using ImageJ to separate IRAK-M staining (red),

246 pigment (brown) and nuclei (blue). Note a nonspecific staining of thickened BM in AMD. (C)
247 Quantification of mean staining intensity of macular area shows more severely reduced IRAK-M
248 expression in both aged and AMD RPE, while the reduced expression in choroid is only significant with
249 old age. There are no changes in retina with ageing or in AMD (n=2 for young control, n=5 for old control
250 and n=11 for AMD). *P < 0.05; ***P < 0.001; ****P < 0.0001; ns, nonsignificant. Comparison by two-
251 way ANOVA (A) or one-way ANOVA (C).

252
253 To further determine any spatial expression of IRAK-M protein within tissue associated with age
254 and AMD, we performed IHC on paraffin-embedded retinal sections of 2 'young' (aged 30 and
255 59y) and 5 'aged' (76-97y) individuals without history of AMD, and 11 AMD patients (76-95y).
256 The paraffin slides were visualized using AP-based IHC due to strong autofluorescence of the RPE
257 that was not fully blocked by Sudan black B quenching. In young samples, IRAK-M (stained in
258 red) was observed in various layers of the retina, RPE and choroid (Non-AMD 59y, Fig. S5A and
259 Fig. 2B). In aged control and AMD samples, the pattern and strength of IRAK-M-immunopositive
260 signals was variable, for example with a heightened signal in OPL/ONL (Non-AMD 97y, Fig. S6B
261 and Fig. 2B), in INL/ONL/IS (inner segment) (Mild AMD 76y, Fig. S5C and Fig. 2B), or in NFL
262 (nerve fiber layer) (Unidentified stage of AMD 85y, Fig. S5D and Fig. 2B). After color
263 deconvolution using Fiji package of ImageJ, the IRAK-M signal (red) and RPE pigment (brown)
264 could be separated and discerned for quantification. Advancing our data in Fig. 1C and D), we
265 identified a marked reduction in IRAK-M expression at the macular RPE and choroid with older
266 age (Fig. 2C). The IRAK-M level of expression was also lower in AMD-macular RPE areas
267 compared to age-matched subjects and was not observed in choroid underlying the macula (Fig.
268 2B and C). Reduction of IRAK-M expression in extramacular tissues was only evident in aged
269 versus young choroid (Fig. S6). Nonspecific staining of Bruch's membrane (BM) for IRAK-M
270 was observed in AMD samples (Fig. 2B) and in negative staining controls. The intensified BM
271 was not evident in non-AMD eyes (38).
272

273 **IRAK-M-deficient mice acquire earlier outer retinal degeneration during ageing**

274 Having established the association between reduced IRAK-M expression and age/AMD, we used
275 IRAK-M-deficient mice (without *Rd8* mutation) to investigate whether ageing and lack of IRAK-
276 M affected outer retinal degeneration. The *Irak3^{-/-}* mouse line bears an IRAK-M mutant, where
277 two-thirds of the pseudokinase domain (exons 9-11) were removed by homologous recombination
278 (36, 39). The multiple conserved cysteine residues within the dimeric structure of the pseudokinase
279 domain of native IRAK-M are essential in the forming of an interactive interface with IRAK4 for
280 the negative regulation of IRAK-Myddosome signaling (40).

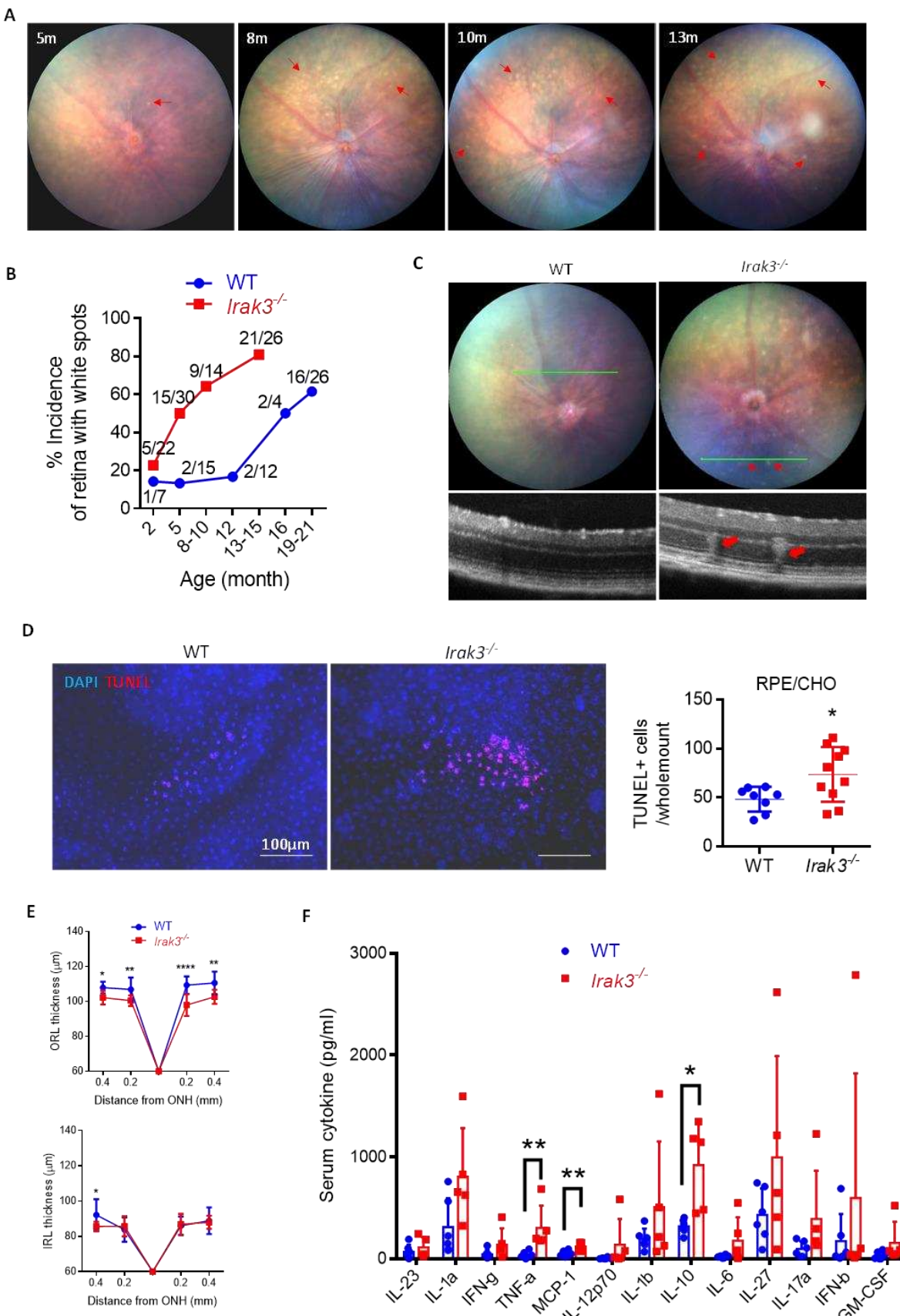
281 Pathological changes were tracked for 15 months using fundoscopy and OCT. Between 2 and 5m
282 of age, there was a sharp increase in the incidence of retinas displaying variable number of fundus
283 white spots, from 22.7% (5 out of 22 eyes) to 50% (15 out of 30) (Fig. S7A, Fig. 3A and B). The
284 fundus spots in mice have been well described as a feature of retinal inflammation linked to
285 accumulated macrophages/microglia in the subretinal space (41, 42). The incidence of abnormal
286 retinal appearance increased and reached 78.6% of eyes (11 out of 14) by 15m (Fig. 3B). Repeated
287 imaging of the same affected retinas showed that the white spots developed with ageing (Fig. 3A).
288 In comparison, WT mice maintained normal retinal appearance (i.e., no progression of white spots)

289 at 12m, however a substantial incidence of WT retinas displayed white spots between 12 and 21m
290 as mice aged (61.5% or 16 out of 26 at 19-21m, Fig. 3B). These time course data demonstrate
291 accelerated ageing-associated retinal abnormalities and degeneration associated with defective
292 IRAK-M (Fig. 3B). Notably, the early appearance of retinal spots was accompanied by outer
293 retinal lesions identified by OCT (Fig. 3C).

294 Increased numbers of CD11b+ myeloid cell populations in the outer nuclear layer (ONL) (Fig.
295 S7B), and CD11b+ cell accumulation in the subretinal space (Fig. S7C) were observed in *Irak3*^{-/-}
296 mice, associated with increased number of apoptotic cells (TUNEL-positive) within the
297 RPE/choroid (Fig. 3D). Although no difference in retinal thickness was found at 5m between WT
298 and *Irak3*^{-/-} mice, the outer retina of *Irak3*^{-/-} mice was significantly thinner by 12-13m (Fig. 3E).
299 In parallel, by 12-13m serum inflammatory cytokine levels in *Irak3*^{-/-} mice were higher than in the
300 WT mice (significant increases in TNF- α , MCP-1 and IL-10; Fig. 3F).

301

Fig. 3



303 **Fig. 3. *Irak3*^{-/-} mice spontaneously display early retinal abnormalities.** (A) Representative fundal images
304 show age-related appearance of white spots (red line arrow) in *Irak3*^{-/-} mouse retinas. (B) Time course of
305 incidence of flecked retina (number of spots > 3) shows increased incidence of retinal spots in *Irak3*^{-/-} mice
306 compared to WT controls. Each value is a ratio of number of flecked retina to total number of retina at each
307 time point. (C) Representative fundal and OCT images demonstrate that the white spots (red line arrow)
308 are associated with outer retinal abnormalities (red arrow) in 5m-old *Irak3*^{-/-} mice. (D) TUNEL staining on
309 RPE/choroidal flatmounts reveals elevated number of apoptotic cells in *Irak3*^{-/-} mice versus WT controls
310 (5m-old) (n=8-10). (E) Quantification of OCT images indicates significant outer retinal thinning in *Irak3*^{-/-}
311 mice aged 12-13m. The change in inner retinal thickness is negligible (n=6-12). (F) Multiplex cytokine
312 array demonstrates an overall higher levels of serum cytokines in *Irak3*^{-/-} compared to WT mice (12-13m-
313 old), where the increases of TNF- α , MCP-1 and IL-10 serum concentrations are statistically significant
314 (n=5-6). *P < 0.05; **P < 0.01; ****P < 0.0001. Comparison by unpaired two-tailed Student's t-test (D) or
315 two-way ANOVA (E and F).

316

317

318 **Oxidative stress reduces RPE-IRAK-M expression and loss of IRAK-M increases 319 susceptibility of outer retina to oxidative damage**

320 Age-associated accumulation of oxidative stress in the RPE is a recognised contributor to the
321 progression of AMD. To examine if oxidative stress could be an independent factor for the
322 reduction of IRAK-M expression, we applied oxidative stressors both *in vitro* and *in vivo*.

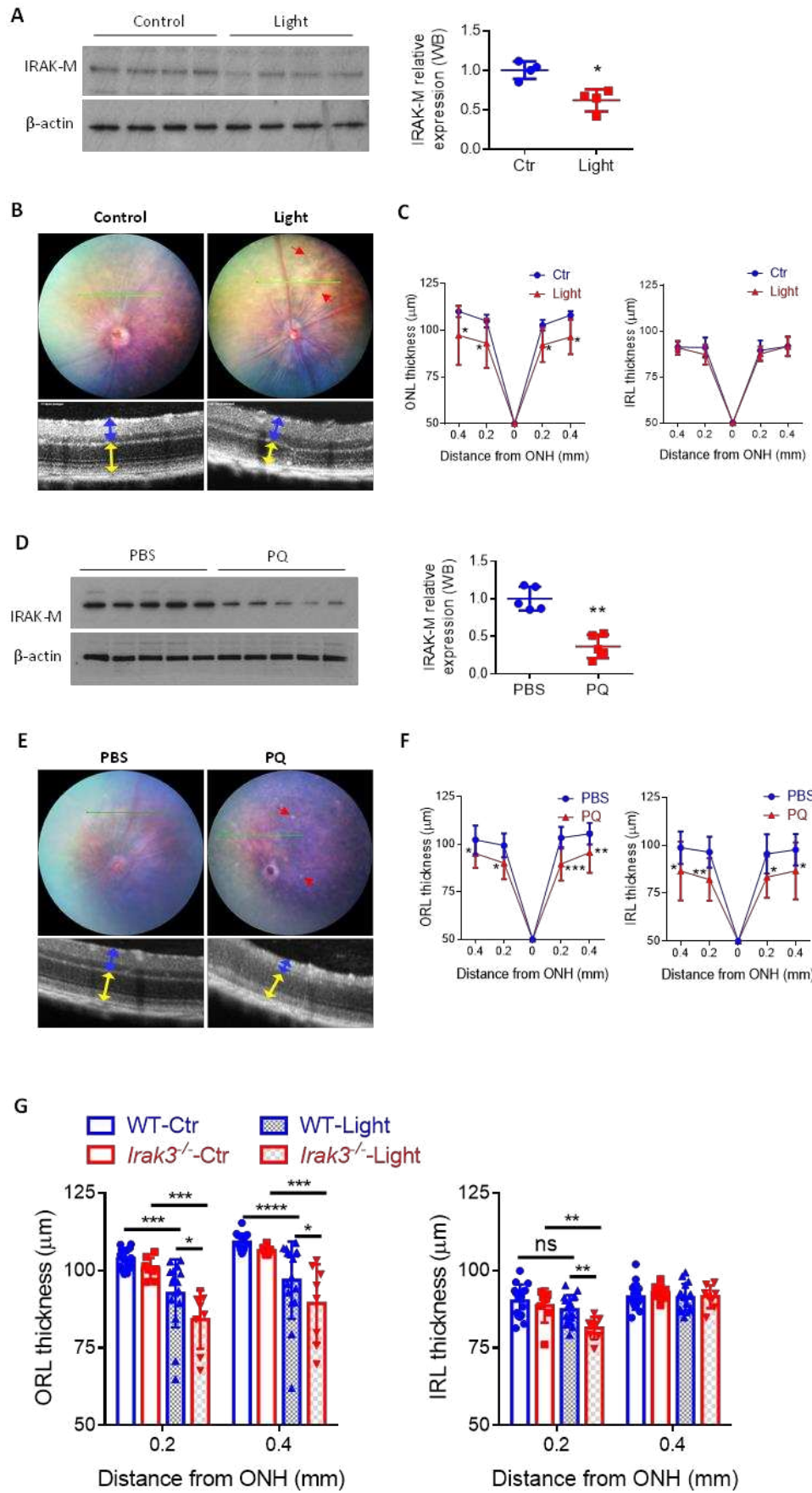
323 *In vitro*, a human ARPE-19 cell line was treated with different doses of paraquat (PQ), a stable
324 chemical primarily inducing mitochondrial ROS, for up to 72h. LDH cytotoxicity assay showed a
325 dose-dependent cytotoxicity caused by PQ exposure for 72h (Fig. S8A), whereas IRAK-M protein
326 expression was suppressed by a sub-toxic dose of PQ (0.25mM) (Fig. S8B). Reduction in IRAK-
327 M was accompanied by an enhanced pro-inflammatory response, demonstrated by the increased
328 secretion of pro-inflammatory cytokines HMGB1, IL-18 and GM-CSF, and decreased secretion
329 of anti-inflammatory IL-11 (Fig. S8C). Likewise, downregulation of IRAK-M expression level
330 following 72h treatment of sub-toxic doses of PQ (0.25-0.5mM) occurred in human iPSC-derived
331 RPE (Fig. S8D-F) and human primary RPE cells (Fig. S8G and H).

332 *In vivo*, retinal oxidative damage was introduced by fundus camera-directed light exposure
333 (100kLux for 20min) (43) or intravitreal administration of PQ (2 μ l at 1.5mM) (44) in C57BL/6J
334 WT mice aged 8w. Western blot analyses showed that IRAK-M expression in the RPE lysate was
335 significantly abated after 7 days in both models (Fig. 4A and D). Fundoscopy and OCT
336 photographs obtained on day 14 displayed the fundal appearance of white spots (red arrows, Fig.
337 4B and E) indicative of accumulated microglia/macrophages inside the ONL (42), alongside
338 thinning of the outer retina indicative of cell loss in the light-induced retinal degeneration (LIRD)
339 model (Fig. 4C), and reduced thickness in both outer and inner retina in the PQ model (Fig. 4F).

340 Given the observed age-dependent increase of retinal pathology in IRAK-M-depleted mice, we
341 next explored whether oxidative stress would exaggerate the effect. Retinal oxidative stress was
342 induced in adult WT and *Irak3*^{-/-} mice (8w old) by light induction. *Irak3*^{-/-} mice exhibited amplified
343 retinal damage compared to WT, particularly a thinner outer retinal layers following light
344 challenge (Fig. 4G).

345

Fig. 4



347 **Fig. 4. Wild-type mice exhibit reduced RPE-IRAK-M expression level by oxidative stress and *Irak3*^{-/-} mice are more vulnerable to light-induced retinal degeneration.** Retinal oxidative stresses were
348 induced in 8-week-old C57BL/6J mice by either fundus-light induction (100kLux for 20min, **A-C**) or
349 intravitreal administration of paraquat (PQ, 2μl at 1.5mM, **D-F**). (**A&D**) Western blot analyses of IRAK-
350 M expression in RPE lysate on day 7 post oxidative damage (n=4 or 5). (**B&E**) Representative fundoscopy
351 and OCT images obtained on day 14 demonstrate appearance of retinal lesions (red line arrows), and
352 reduced thickness of outer retina (yellow double-arrow lines) in light model (n=8, **C**), or both outer and
353 inner retina (blue double-arrow lines) in PQ model (n=9-11, **F**). (**G**) Eight-week-old WT and *Irak3*^{-/-} mice
354 were subjected to retina oxidative insults by light induction. OCT quantification of retinal thickness
355 (average of temporal and nasal measurements) demonstrates exaggerated retinal thinning in *Irak3*^{-/-} mice
356 compared to WT controls on 14 days post light induction, which is more pronounced in outer retinal layers
357 (n=8-16). *P < 0.05; **P < 0.01; ***P < 0.001; ****P < 0.0001. Comparison by unpaired two-tailed
358 Student's t-test (A and D) or two-way ANOVA (C, F and G).

360

361

362 AP-1 regulates IRAK-M expression in RPE cells in age-dependent manner

363 Known transcription factors regulating IRAK-M expression in monocytes or lung epithelial cells
364 include activation protein 1 (AP-1) and CCAAT/enhancer-binding protein beta (C/EBP-β) (45,
365 46). By analysing human RPE/choroidal lysate derived from donor eyes without recorded ocular
366 disease, we found that along with age-associated reduction in IRAK-M level, expression of c-Jun,
367 an AP-1 subunit, was decreased in aged samples compared to young controls (Fig. S9A and B). c-
368 Fos, another AP-1 subunit, was reduced in old age compared to middle-age samples (Fig. S9A and
369 B). C/EBP-β expression had no change during ageing process.

370 The association of c-Jun and c-Fos with the IRAK-M promoter region were confirmed by ChIP
371 assay on ARPE-19 cells, and this was significantly enhanced in response to LPS stimulation for
372 24h (Fig. S9C). To investigate whether oxidative stress altered AP-1 activity or expression in the
373 RPE, we treated ARPE-19 cells with PQ and demonstrated a dose-dependent downregulation of
374 phosphorylation of both c-Jun and c-Fos after 72h, while total c-Jun and c-Fos expression were
375 downregulated by higher dose of PQ (Fig. S9D and E). Through inhibition of AP-1 subunit activity
376 and expression, SP600125 (primarily targeting c-Jun) and T5224 (targeting c-Fos) at 20 μM
377 significantly decreased IRAK-M expression (Fig. S9D and E). Consequently, treatment with AP-
378 1 inhibitors resulted in enhanced ARPE-19 susceptibility to PQ-induced cytotoxicity (Fig. S9F),
379 similar to the observed effect induced by IRAK-M siRNA (Fig. S9G). Increasing c-Jun expression
380 via CRISPR/Cas9 activation plasmid upregulated IRAK-M expression (Fig. S9H). The effect on
381 suppressing oxidative stress-induced cytotoxicity by overexpressing IRAK-M using
382 CRISPR/Cas9 activation plasmid transfection was not found when c-Jun expression was
383 augmented (Fig. S9H).

384

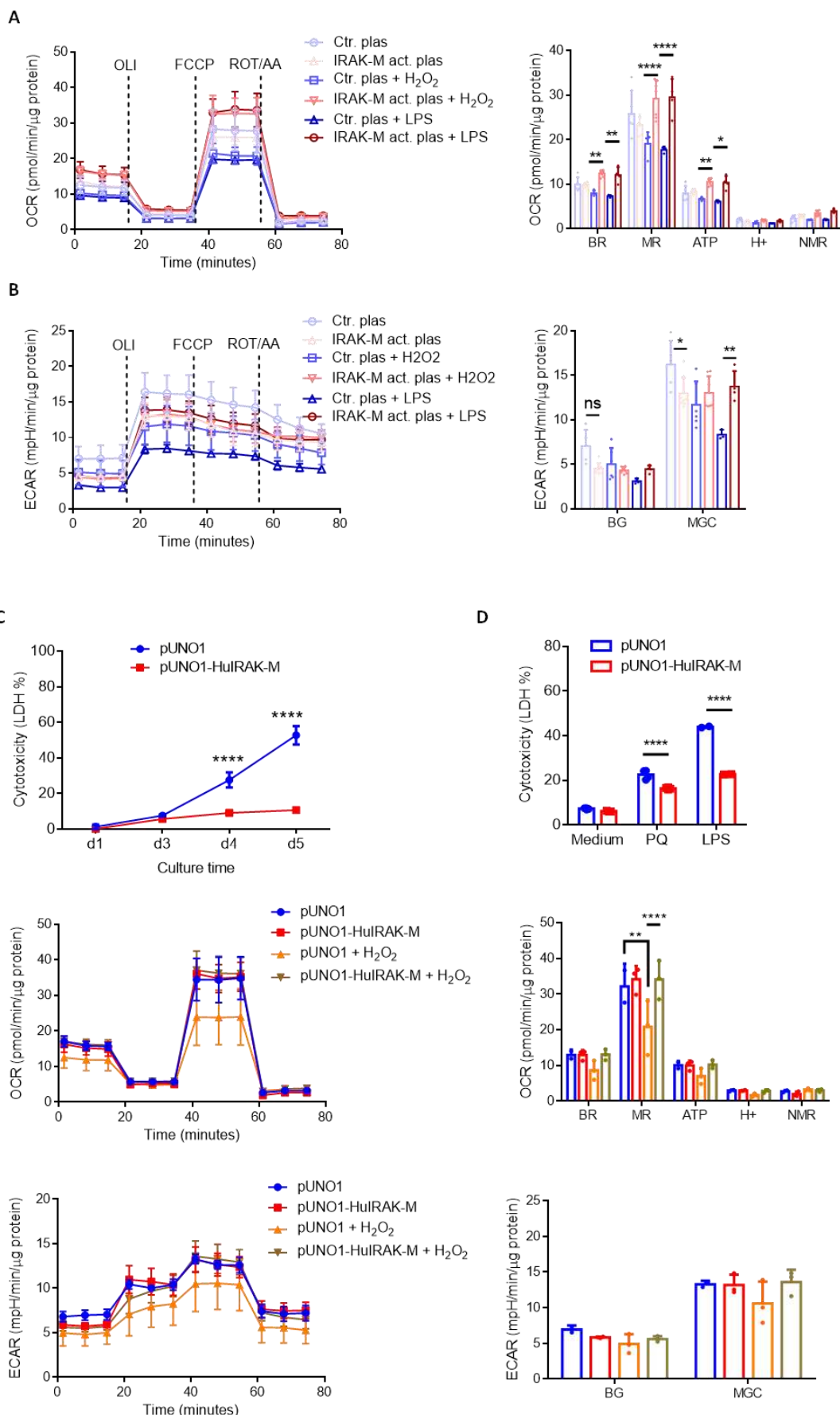
385 IRAK-M deficiency induces RPE mitochondrial dysfunction and senescent phenotype which 386 is protected by IRAK-M augmentation

387 To elucidate metabolic mechanisms involved in IRAK-M deficiency-induced retinal degeneration,
388 we examined RPE cell metabolism and senescence using primary mouse RPE cells. IRAK-M-
389 deficient cells showed reduced levels of basal mitochondrial respiration (BR) and ATP production
390 compared to WT cells as assessed by OCR analyses (Fig. S10A), while no significant differences

391 in basal glycolysis (BG) and maximal glycolytic capacity (MGC) were observed between
392 genotypes as assessed by ECAR (Fig. S10B). These data infer a role of IRAK-M in the
393 maintenance of mitochondrial function in RPE cells. In support of this, *Irak3*^{-/-} RPE cells were
394 more prone to oxidative stressor (PQ or H₂O₂)-induced senescent phenotype, marked by increased
395 SA- β -gal activity (Fig. S10C), enhanced expression of cyclin-dependent kinase inhibitor p21^{CIP1},
396 decreased nuclear lamina protein LB1 (Fig. S10D), and elicited secretion of IL-6 (a senescence-
397 associated cytokine) (17) (Fig. S10E). The basal secretion level of pro-inflammatory cytokine
398 HMGB1 of *Irak3*^{-/-} RPE cells was significantly higher than the WT cells but the responsiveness to
399 the oxidative stressors were comparable (Fig. S10F).

400 Based upon the data above demonstrating a role of IRAK-M in the context of ageing and oxidative
401 challenge, we examined whether an overexpression of IRAK-M could protect RPE. Native IRAK-
402 M expression in human iPSC-derived RPE cells was augmented via transfection of a
403 CRISPR/Cas9-based activation plasmid (Fig. S11A). After 48h of transfection, the cells were
404 treated with H₂O₂ or LPS for a further 24h. OCR analysis demonstrated that basal and maximal
405 mitochondrial respiration were both sustained by IRAK-M overexpression, but impaired in sham-
406 transfected cells following oxidative or immune stresses (Fig. 5A). Although untreated IRAK-M-
407 overexpressing iPSC-RPE cells displayed lower maximal glycolytic activity than control plasmid-
408 transfected cells, the level remained stable upon H₂O₂ or LPS treatment (Fig. 5B). In contrast,
409 glycolytic activity in control cells was significantly reduced by 24h treatment with H₂O₂ or LPS
410 (Fig. 5B). The lower level of glycolysis in un-stressed iPSC-RPE with overexpressed IRAK-M
411 suggests less bio-energetic dependency on glucose, with possible benefits to glucose-dependent
412 photoreceptors (47).

Fig. 5



414 **Fig. 5. Overexpression of IRAK-M in RPE cells supports metabolic activities and inhibits cell death**
415 **against stressors. (A&B)** Metabolic flux analyses demonstrate that increasing endogenous IRAK-M
416 expression in human iPSC-RPE cells via CRISPR/Cas9 activation plasmid maintains both mitochondrial
417 respiration (OCR, **A**) and glycolytic capacity (ECAR, **B**), upon 24h treatment with 30 μ M H₂O₂ or 1 μ g/ml
418 LPS (n=3-7). **(C)** Stably transfected cell lines selected from mouse B6-RPE07 cells were established to
419 persistently express human IRAK-M. Time course of LDH release over 5 days since confluence of
420 monolayers shows sustained cell viability by human IRAK-M transfection (n=4-8). **(D)** Human IRAK-M
421 expression inhibits PQ (125 μ M) or LPS (40 ng/ml)-induced cytotoxicity post 72h of treatment in stably
422 transfected B6-RPE07 cells (n=2-4). **(E&F)** Primary mouse *Irak3*^{-/-} RPE cells were subjected to transient
423 transfection for human IRAK-M expression using pUNO1 plasmid and 48h later, the cells were treated
424 with 60 μ M H₂O₂ for another 24h. OCR analysis (**E**) shows protected mitochondrial maximal respiration
425 by human IRAK-M against oxidative stress treatment. ECAR analysis (**F**) does not show any changes in
426 glycolysis activity by H₂O₂ treatment or IRAK-M transfection (n=3). *P < 0.05; **P < 0.01; ****P <
427 0.0001; ns, nonsignificant. Comparison by two-way ANOVA.

428
429 ARPE-19 cells with IRAK-M overexpression induced by CRISPR/Cas9 partially reversed LPS-
430 induced reduction in maximal mitochondrial respiration (Fig. S11B and C), supporting the
431 findings from human iPSC-RPE cells (Fig. 5A). Taken further, overexpression of IRAK-M in
432 ARPE-19 promoted the formation of autophagosomes (LC3B-GFP) and autolysosomes (LC3B-
433 RFP) following H₂O₂ or LPS treatment, suggesting an upregulated autophagy flux (Fig. S11D).
434 Moreover, ARPE-19 senescence induced by sub-toxic dose PQ (0.25 mM) was prevented by
435 IRAK-M overexpression, as we documented decreased SA- β -gal activity and HMGB1 secretion
436 (Fig. S11E and F). Finally, a marked LDH release induced by a toxic dose of PQ (1 mM) was
437 significantly subdued by increasing IRAK-M expression (Fig. S11G).

438 We then created stably transfected RPE cell lines maintained in selective medium from a parent
439 mouse B6-RPE07 cell line that expressed either mouse or human *IRAK3* mRNA (Fig. S12A).
440 Expression of mouse *Irak1* and *Irak4* were not affected. A NF- κ B activity assay showed a decrease
441 in DNA-binding activity of nuclear NF- κ B in human *IRAK3*-expressing mouse cells after LPS
442 stimulation (Fig. S12B), demonstrating that the transduced human *IRAK3* is as functional as its
443 murine counterpart in suppressing NF- κ B activation in mouse RPE. Stably transfected RPE cells
444 overexpressing human *IRAK3* survived longer, compared to sham-transfected cells when assessing
445 cell death after four days of confluence (Fig. 5C). Freshly confluent cells (with stable
446 overexpression of *IRAK3*) exhibited a reduced stressor-induced cytotoxicity after treatment with
447 PQ (0.125 mM) or LPS (40 ng/ml) for 3 days (Fig. 5D). To exclude the possible contribution of
448 native mouse *Irak3* to cell response observed, we performed transient transfection on primary RPE
449 cells isolated from *Irak3*^{-/-} mice. A metabolic flux assay was applied to examine metabolic
450 alterations in response to shorter period of treatment with H₂O₂ (24h, Fig. 5E and F). Similar to
451 data from human iPSC-RPE cells using CRISPR/Cas9 activation plasmid (Fig. 5A and B),
452 maximal mitochondrial respiration in mouse primary *Irak3*^{-/-} RPE cells was retained by human
453 *IRAK3* transduction after H₂O₂ treatment (Fig. 5E). H₂O₂ -induced oxidative stress had no effect
454 on glycolysis in *Irak3*^{-/-} RPE cells (Fig. 5F).

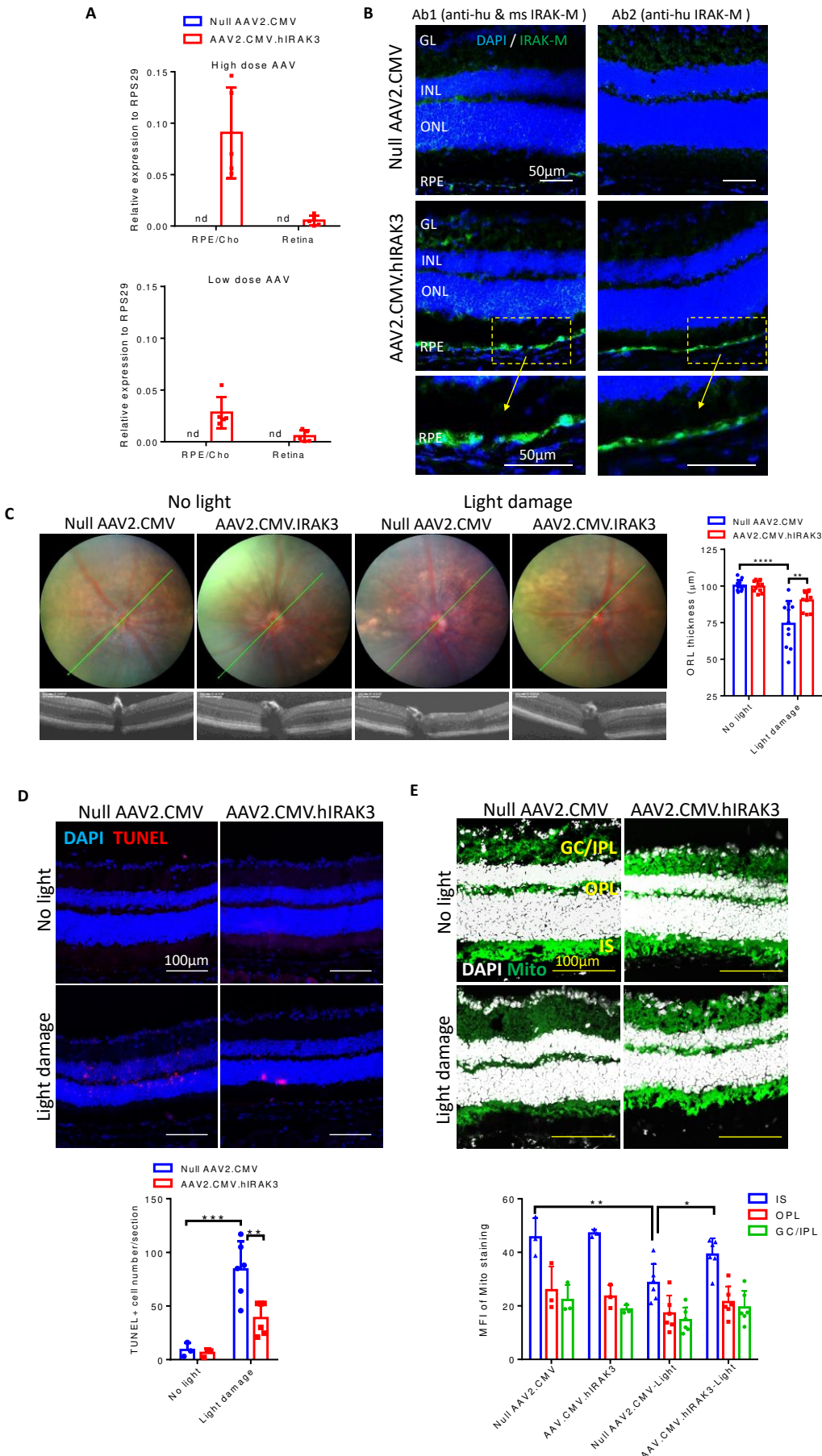
455
456

457 **AAV2-mediated IRAK-M expression suppresses light-induced retinal degeneration in wild-
458 type mice and spontaneous retinal degeneration in *Irak3*^{-/-} mice**

459 To correct defective gene expression or function in diseases, experimental approaches have
460 included introducing human genes, such as *RPE65*, *CFH* and *ND4* (NADH dehydrogenase subunit
461 4), to mouse eyes for functional or preclinical evaluation (48-51). Such studies have utilised AAV2
462 and translated to clinical trials to treat RPE-related eye diseases (52). To identify the dose-
463 dependent transduction efficacy, 2 μ l of AAV2 encoding EGFP under the control of constitutive
464 cytomegalovirus (CMV) promoter (AAV2.CMV.EGFP) at 1×10^{12} or 2×10^{11} gc/ml were delivered
465 into mouse eyes via the subretinal route. The ‘high dose’ (1×10^{12} gc/ml in 2 μ l, or 2×10^9 gc/eye)
466 induced a more pronounced EGFP expression 2-11 weeks post the injection than the “low dose”
467 (2×10^{11} gc/ml or 4×10^8 gc/eye) (Fig. S13A). Administration with AAV2.CMV.hIRAK3 induced
468 a dose-dependent *IRAK3* mRNA expression in RPE/choroid two weeks post injection, compared
469 to a similar vector but with no transgene used as a control ‘null’ vector (Fig. 6A). Transduced
470 human IRAK-M protein was detected in the RPE, as demonstrated by immunohistochemistry,
471 using two independent IRAK-M antibodies (Fig. 6B).

472 To evaluate the protective effects of IRAK-M transgene expression *in vivo*, we applied light-
473 induced retinal degeneration in mice 2 weeks after AAV injection (2×10^9 gc/eye). Light exposure
474 of the null AAV2-injected eyes resulted in a decrease of outer retinal thickness, indicative of the
475 PR loss. The protective effect of AAV2.CMV.hIRAK3 treatment from PR injury was conspicuous,
476 as demonstrated by suppression of light-induced outer retinal thinning (Fig. 6C). The LIRD model
477 exhibited significant outer retinal thinning (Fig. 4C), supported by TUNEL+ apoptosis in the ONL
478 (Fig. 6D). There were fewer number of TUNEL+ cells within inner retinal layers, indicating a
479 secondary cell death response in the inner retina following PR loss (53, 54). Contemporaneous
480 with the retaining of retinal thickness by AAV.IRAK3 was a reduction in light-induced TUNEL+
481 cell apoptosis within retinal sections (Fig. 6D), as well as an inhibition of mitochondrial
482 impairment in the IS (Fig. 6E). The mitochondria in GL, IPL and OPL were less affected by light
483 challenge (Fig. 6E).

Fig. 6



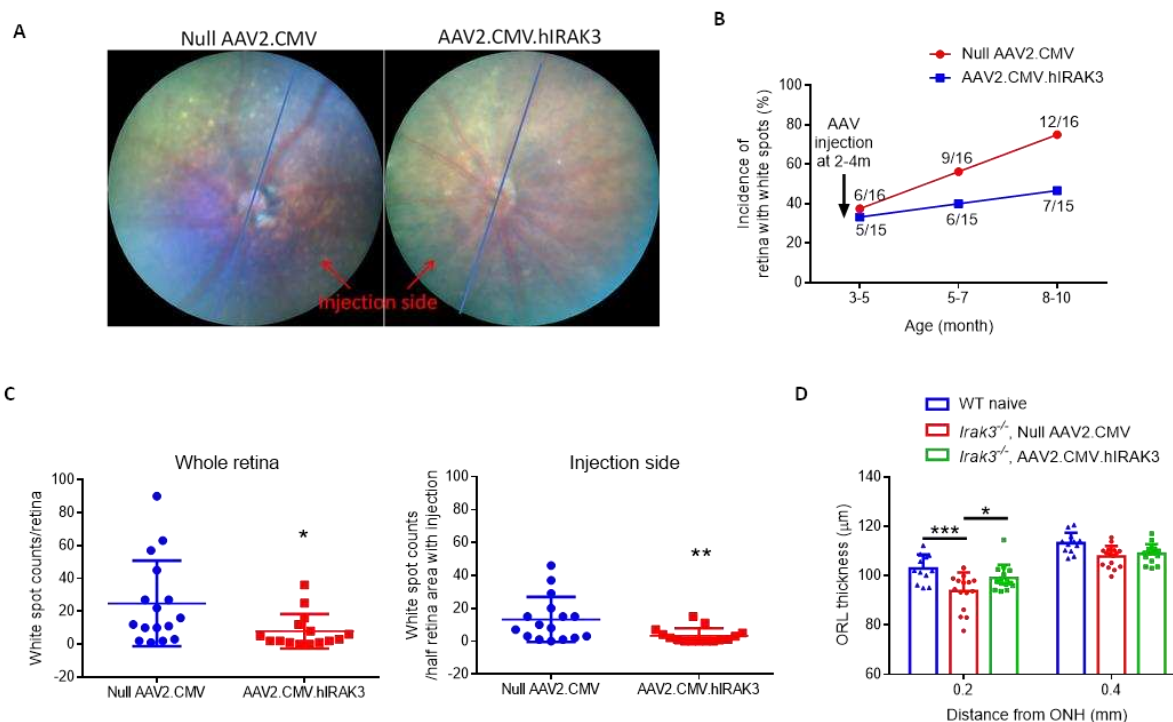
485 **Fig. 6. Subretinal delivery of AAV.hIRAK3 protects retina against light damage in wild-type mice.**
486 (A) Two weeks post subretinal injection of AAV2.CMV.hIRAK3 or AAV2.CMV (high dose 2×10^9 versus
487 low dose 4×10^8 gc/eye), RPE/choroid and retina were analyzed for IRAK3 transgene expression using qRT-
488 PCR, normalized by RPS29 mRNA (n=5). (B) Retinal cryosections were examined for high dose AAV-
489 mediated IRAK-M expression using an antibody recognizing both human and mouse IRAK-M (Ab1), or
490 an antibody specific to human IRAK-M (Ab2). Representative confocal images were shown. (C-E) Two
491 weeks after subretinal injection with the high dose of AAV2.CMV.hIRAK3 or null vector, each mouse was
492 subjected to light-induced retinal degeneration in one eye and left thereafter for a further two weeks,
493 followed by assessment of retinal pathology and therapeutic response. (C) Representative fundoscopy/OCT
494 images and quantification show light-induced retinal lesions and averaged outer retinal thickness (n=10-
495 11). (D) Representative confocal images of TUNEL staining on retinal sections and quantification of 3
496 sections from each eye (n=3-6). (E) Confocal images of MitoView Green staining for mitochondrial content
497 and MFI measurement in 3 different fields from two sections of each eye (n=3-6). *P < 0.05; **P < 0.01;
498 ***P < 0.001; ****P < 0.0001. Comparison by two-way ANOVA.

499

500 Based upon our finding that *Irak3*^{-/-} mice developed signs of retinal degeneration earlier than WT,
501 we asked whether AAV-IRAK3 could attenuate outer retinal degeneration caused by IRAK-M
502 deficiency and ageing. To this end, we performed subretinal administration of
503 AAV2.CMV.hIRAK3 or null AAV2.CMV (2×10^9 gc/eye) in young *Irak3*^{-/-} mice (2-4m old) and
504 allowed them to age. Six months following the subretinal delivery of AAV vectors, we found that
505 AAV2.CMV.hIRAK3 blunted the age-dependent occurrence of retinal spots (Fig. 7A and B), and
506 significantly reduced the number of retinal spots in aged *Irak3*^{-/-} mice compared to the null vector
507 (8-10m old; Fig. 7C). The effect was more pronounced within the treatment side of the retina
508 receiving the vector, as expected (Fig. 7C). Importantly, compared to the null AAV treated mice,
509 AAV-IRAK3 delivery showed attenuated outer retinal thinning (Fig. 7D).

510

Fig. 7



511

512 **Fig. 7. Subretinal delivery of AAV.hIRAK3 prevents from age-related spontaneous retinal**
513 **degeneration in *Irak3*^{-/-} mice.** 2×10⁹ gc of AAV2.CMV.hIRAK3 was injected subretinally in one eye of
514 each *Irak3*^{-/-} mouse (2-4m old), with null vector injected to the contralateral eye. Mice were then monitored
515 by fundoscopy and OCT for 6 months thereafter. (A) Representative fundal images show retinal spots in
516 8m-old *Irak3*^{-/-} mice with AAV administration at the age of 2m. Blue lines separate the retina into two sides
517 based on the injection site. (B) Time course of incidence of flecked retina shows IRAK3 gene therapy
518 decelerated the appearance of retinal spots in ageing *Irak3*^{-/-} mice (n=15 or 16). (C) Number of retinal spots
519 in whole retina or at the injection side, was blind-counted for comparison between AAV2.CMV.hIRAK3
520 and null vector groups (8-10m-old, n=15 or 16). (D) OCT quantification shows a reduction in outer retinal
521 thickness close to the centre region (0.2 mm distant from optic nerve head) in 8-10m-old *Irak3*^{-/-} mice
522 compared to age-matched WT littermates, which is revoked by AAV.hIRAK3 gene delivery (n=12-16). *P
523 < 0.05; **P < 0.01; ***P < 0.001. Comparison by unpaired two-tailed Student's t-test (C) or two-way
524 ANOVA (D).

525

526

527 DISCUSSION

528 Among the plethora of pathways implicated in AMD, there is a strong association and evidence
529 base for a central role of altered immune responses and innate immune dysregulation alongside
530 pro-degenerative stressors, such as oxidative stress and metabolic perturbation. In the present
531 study, we have demonstrated a protective role of the immune regulator IRAK-M in the metabolic
532 and immune homeostasis of the RPE. This is based on the expression levels of IRAK-M in young,
533 old and AMD human eyes, genetic variant burden in those with AMD and experimental models
534 of oxidative stress, ageing and IRAK-M deficiency. A feed-forward loop with ageing, oxidative
535 stress and expression decline of the immune regulator, IRAK-M, may constitute a pro-
536 inflammatory microenvironment driving retinal degeneration. Replenishing the homeostatic
537 regulator IRAK-M maintains mitochondrial function, inhibits pro-inflammatory senescence and
538 promotes cell survival, therefore protecting the retina from degeneration in a LIRD model and
539 progressive degeneration in *Irak3*^{-/-} mice. As we observed, IRAK-M is consistently reduced with
540 ageing, oxidative stress and AMD; the replenishment of IRAK-M may be a broadly applicable
541 therapeutic strategy for treating AMD patients.

542 Prior work has noted the expression of IRAK-M in cells other than monocytes/macrophages,
543 including airway and intestine epithelium, fibroblasts, neurons, neutrophils, dendritic cells
544 basophils and B cells (36, 55, 56). In lung biopsy samples from healthy humans, IRAK-M is highly
545 expressed in type II epithelial cells and the dysfunction of IRAK-M is implicated in inflammatory
546 lung diseases (31). Tarallo *et al.* reported aberrant activation of NLRP3-inflammasome and
547 Myddosome signaling, such as increased phospho-IRAK1/4 levels in RPE lysates of GA patients,
548 albeit without probing the regulator IRAK-M (16). Here we report that the expression of IRAK-
549 M declines with age in the RPE but not retinal tissue and is reduced further in AMD subjects
550 compared to age-matched controls (Fig. 1, 2, S2, S3, S4 and S6). Additionally, we found that
551 IRAK-M was expressed by bilayer ciliary epithelium (Fig. S1G and H), indicating the distribution
552 of this key inflammation inhibitor in other ocular epithelium barriers. The RPE regulates and
553 protects against excessive oxidative stressors, inflammasome activation, mitochondrial
554 impairment, lipid accumulation and cellular senescence (4, 17, 26, 57), all pathways that can
555 propel the insidious AMD progression (13, 14). TLRs (TLR1-7, 9 and 10) are expressed by RPE
556 cells and IL-1Rs are ubiquitously distributed (58). Coupled with the known immunosuppressive
557 factors produced by the RPE, such as membrane molecules CD200, IL-1R2, IL-1Ra, FasL, and
558 anti-inflammatory chemokines or cytokines (CX3CL1, TGF-β, IL-11 and IFN-β) (23, 59-62),
559 IRAK-M is required for balancing the regional innate and adaptive immune activation and
560 suppression at the posterior segment of the eye. We showed that *Irak3*^{-/-} mice incurred greater
561 oxidative damage, including RPE cell mitochondrial dysfunction, pro-inflammatory senescence,

562 and early AMD-like pathologies such as subretinal accumulation of myeloid cells, outer retinal
563 lesions, and cell death (Fig. 3, 4G, S7 and S10). Additionally, *Irak3*^{-/-} mice displayed systemic
564 inflammation evidenced by increased serum cytokine levels.

565 The downregulation or upregulation of IRAK-M expression is context-dependent. For instance,
566 upregulation of IRAK-M was identified following ischemia-reperfusion of liver and brain (63,
567 64), and in infarcted heart (65), where it is thought to limit the magnitude of immune responses
568 and repair pro-inflammatory damage. In a mouse model of cerebral ischemia, IRAK-M was found
569 to be induced by HIF1 α and played a neuroprotective role by inhibition of NF- κ B signaling and
570 production of COX-2, TNF- α , NLRP3 and iNOS. In comparison, *IRAK3*^{-/-} mice developed
571 exacerbated infarcts (58). In contrast to acute responses, downregulation of IRAK-M was more
572 associated with chronic diseases, exemplified by alcoholic liver disease, inflammatory bowel
573 disease, insulin resistance and metabolic syndrome (25, 29, 30). Indeed, whilst acute alcohol intake
574 increases IRAK-M expression in human monocytes, chronic alcohol exposure results in its
575 decrease in expression and enhanced inflammation (66). In obese subjects, reduced IRAK-M
576 levels in monocytes and adipose tissues constitute a causative factor of mitochondrial oxidative
577 stress and systemic inflammation (30). Furthermore, age-related decreases in the basal level of
578 IRAK-M and its inducibility upon TLR activation have been discovered in PBMCs and fibroblasts
579 in rodents (67, 68). Using RNA-Seq, Western blot and IHC, we localized the decline in IRAK-M
580 expression to the RPE, rather than of the retina or choroid, in ageing, oxidative stress and AMD
581 (Fig. 1C-D, 2A-C, 4A-B, S2, S3B), indicating that RPE-IRAK-M serves as an early harbinger
582 molecule of degeneration progressing to AMD. Increasing IRAK-M in the RPE *via* boosting
583 endogenous gene expression or exogenous gene delivery helped to maintain cell functions
584 (mitochondrial activity and autophagy) and inhibit cellular senescence and NF- κ B activity (Fig. 5,
585 S11 and S12), implying the importance of IRAK-M for the RPE health (Fig. 6 and 7).

586 Reduced IRAK-M expression with age may be a repercussion of the pathophysiological processes
587 in the genomic or epigenomic programmes. Our data show an association of reduced AP-1 subunit
588 proteins c-Jun and c-Fos and decreased IRAK-M expression (Fig. S9). This agrees with the
589 findings that aged human fibroblasts display declined c-Jun and c-Fos proteins, a shifted
590 distribution of AP-1 components and DNA binding capacity (69). Decreased transcription activity
591 of AP-1 has been linked to tissue and cell ageing (70, 71), as opposed to NF- κ B which was
592 frequently increased in activity in aged tissues and age-related illnesses such as Alzheimer's
593 disease, diabetes and osteoporosis (71, 72). A recent genome-wide profiling study indicated that
594 AP-1 functioned as a governing agent in the senescence programme by shaping the enhancer
595 landscape and determining the dynamic hierarchy of the transcription factor network leading to
596 senescence (73). In our work, AP-1 inhibition in human ARPE-19 cells and IRAK-M-deficient
597 murine primary RPE cells rendered the cells more susceptible to oxidative stress-induced
598 cytotoxicity and/or senescence. Of note, and possibly due to the miscellaneous functions of AP-
599 1/c-Jun signalling in stress response and apoptosis (74, 75), increasing c-Jun expression or activity
600 had no beneficial effect on oxidative damage protection (Fig. S9H).

601 Limitations exist in this study and further investigations will enable a deeper mechanistic
602 understanding of retinal degeneration and help inform potential therapeutic approaches. Our *in*
603 *vivo* assessment did not reveal any ocular toxicity when overexpressing IRAK-M for more than 6
604 months in *Irak3*^{-/-} mice. However, for translation assessment, large animal studies will be required.
605 We overexpressed IRAK-M by different methods, including CRISPR activation and plasmid- or
606 AAV-based gene delivery, and observed benefits. Future studies should determine levels of IRAK-
607 M expression to define the dose-response curve and further interpret the role of IRAK-M
608 regulation and levels of AP-1 activity (29).

609 In conclusion, we have identified an age-related diminishment of IRAK-M expression largely
610 restricted to the RPE, which is worsened in AMD. Our findings offer insights into a previously

611 unrecognized mechanism where IRAK-M plays a crucial role to maintain RPE cell homeostasis
612 and function via co-targeting mitochondrial health, oxidative stress, autophagy and inflammation.
613 As a consequence, gene augmentation of IRAK-M demonstrates translational benefit in
614 counteracting side-effects of ageing or oxidative stress and reducing outer retinal degeneration in
615 disease models. Given the complexity of multiple affected pathways in AMD, a therapeutic
616 strategy via manipulating IRAK-M in the RPE to address multiple pathways is potentially
617 applicable in a wider population of AMD patients.

618

619

620 MATERIALS AND METHODS

621 Study Design

622 The overall goals of this study were to define whether alteration of IRAK-M expression in RPE
623 during the ageing process and in AMD occurs. The subsequent goal was to develop a targeted gene
624 therapy for age-related and inflammation-driven RPE and retinal degeneration. The primary
625 experimental procedures are described below, with detailed Materials and Methods listed in the
626 Supplementary Materials.

627 *Human sample analyses*

628 For investigations on human ocular samples in all respective institutions, experiments were
629 conducted according to the Declaration of Helsinki principles and in compliance with approved
630 institutional guidelines. We used gene burden test on the large-scale genetic data from
631 International AMD Genomics Consortium (IAMDGC) that contains 16,144 late AMD cases
632 versus 17,832 age-matched controls (6) to analyze whether there was a genetic association between
633 rare protein-altering variants of IRAK-M and AMD, compared to other Myddosome-associated
634 proteins. Human age-related progressive changes in mRNA expression of IRAKs were probed in
635 samples including 227 extramacular; 159 macula RPE/choroid and 238 extramacular; 242 macula
636 retina 6 mm trephine tissue punches, by Affymetrix chip-based Microarray and linear regression
637 analysis. Age-related change of IRAK-M expression in RPE/choroid at the protein level was
638 determined by Western blot using postmortem eye tissues from young, middle-aged and aged
639 groups with mixed genders (4-6 samples per age group). AMD-associated changes in mRNA
640 expression of IRAKs and known genes involved in the negative regulation of TLR/IL-
641 1R/MyD88/IRAK1/4 signalling pathways were discerned by data mining of RNA-Seq data
642 (GSE99248), containing 8 AMD donor eyes aged 83-95 years versus 7 control donor eyes aged
643 83-92 years. AMD-associated IRAK-M protein expression change was examined by
644 immunohistochemistry of postmortem eye sections from 11 individuals with varying stages of
645 AMD pathology (aged 76-95 years, mixed gender) and 5 age-matched control subjects without
646 recorded eye disorders (aged 76-97 years, mixed gender). The processing and staining of all
647 sections were executed at the same time with the same vials of reagents and antibody to avoid
648 batch effects.

649 *Irak3^{-/-}, ageing mice and oxidative stress induction*

650 We used *Irak3^{-/-}* and WT mice to define whether ageing and/or lack of IRAK-M affected outer
651 retinal degeneration. As the original *Irak3^{-/-}* breeding pairs purchased from Jackson Laboratory
652 (strain B6.129S1-Irak3tm1Flv/J, stock no. 007016) presented Rd8 mutation of Crb1 gene that was
653 not reported previously, the mice were backcrossed with WT C57BL/6J for selection of Rd8-
654 negative *Irak3^{-/-}* genotype (76). Only male mice from the established Rd8-negative *Irak3^{-/-}* colony
655 were used to avoid possible sex-associated variation in immune responsiveness (77). All animal

656 experiments were approved by the University of Bristol Ethical Review Group and conducted in
657 accordance with the approved institutional guidelines. Time course of clinical examinations on
658 retinal pathology, including retinal structure, fundus spots and thickness, was performed using
659 Micron IV-guided fundoscopy and optical coherence tomography (OCT) in *Irak3^{-/-}* mice (aged 2-
660 15 months) and WT mice (aged 2-21 months). Primary endpoints were RPE cell death, subretinal
661 accumulation of macrophages, and serum cytokine concentrations at indicated time points. To
662 determine whether oxidative stress could be an independent factor affecting IRAK-M expression,
663 we applied oxidative stressors to different RPE cells *in vitro* and 8-week-old WT mice *in vivo*. The
664 mice were subject to fundus camera-directed light exposure (100kLux for 20min) (43) or
665 intravitreal injection of paraquat (2 μ l at 1.5mM) (44). The contralateral eye was left without light
666 challenge or injected intravitreally with PBS as a control. The sample size was chosen empirically
667 based on the results of previous studies, which varied between experimental settings. In general,
668 4-30 replicates for each condition were used per time point or experiment, with precise numbers
669 specified in the figure legends.

670 To elucidate metabolic mechanisms involved in IRAK-M deficiency-induced retinal degeneration,
671 we isolated primary RPE cells from 5-month-old *Irak3^{-/-}* versus WT littermates and characterized
672 cell metabolism and senescent phenotype. To demonstrate whether IRAK-M had a protecting role
673 for RPE cells against oxidative or immune challenges *in vitro*, we overexpressed IRAK-M by
674 either endogenous CRISPR activation or exogenous IRAK-M delivery via plasmid vectors. *In*
675 *vitro* cell responses to stressors and IRAK-M gene delivery were assessed for mitochondrial
676 respiration and glycolytic activities, autophagy flux, cytokine secretion, and expression of
677 senescence markers.

678 ***Therapeutic approaches***

679 We undertook *in vivo* therapeutic evaluation of IRAK-M replenishment via subretinal
680 administration of AAV2-expressing human IRAK-M in two different murine models of retinal
681 degeneration, light-induced outer retinal degeneration in young WT mice and spontaneous outer
682 retinal degeneration in ageing *Irak3^{-/-}* mice. In both models, null AAV2 vehicle injections served
683 as a negative control to determine baseline responses. The control AAV2 and IRAK3-expressing
684 AAV2 were both under the control of constitutive cytomegalovirus (CMV) promoter. A pilot
685 experiment to determine viral dose-dependent transduction efficacy was performed by subretinal
686 injection of 2 \times 10⁹ gc (high dose) or 4 \times 10⁸ gc (low dose) of AAV2.CMV.EGFP to each eye and
687 evaluated by fundal fluorescence imaging for 11 weeks. AAV-mediated human IRAK-M
688 transgene expression in mice RPE/retina was verified by qPCR and immunohistochemistry of
689 retinal samples. For the light model, retinas were exposed to light challenge at two weeks post
690 AAV injection, and retinal pathologies were examined after a further two weeks by fundoscopy,
691 OCT, and histology for TUNEL+ cell death and mitochondrial content. For the *Irak3^{-/-}* model, we
692 monitored *Irak3^{-/-}* mice (2-4m old) for 6 months following subretinal injection of AAV vectors
693 using quantitative parameters such as retinal fundus spots and outer retinal thickness, measured by
694 fundoscopy and OCT. Laterality of injected eyes was randomized, and the investigators were
695 blinded to the vector type throughout intervention and analysis.

696

697 **Statistics**

698 Results are presented as means \pm standard deviation (SD). A simple linear regression was utilized
699 to analyze the correlation between gene expression and human ageing using Microarray data.
700 Statistical analysis was performed using an unpaired two-tailed Student's t-test between two
701 groups. Tests for normal distribution and homogeneity of variance and comparisons between more
702 than two groups were conducted using one-way ANOVA. A two-way ANOVA was used to assess

703 the interrelationship of two independent variables on a dependent variable, followed by the
704 Kruskal–Wallis test with Bonferroni correction for *post hoc* comparisons. Differences between
705 groups were considered significant at $P < 0.05$. Statistical analyses were conducted using
706 GraphPad Prism 8.0.

707

708 **List of Supplementary Materials**

709 Materials and Methods

710 References (1-10)

711 Table S1

712 Fig. S1 to S13

713

714

715 **REFERENCES**

1. J. Moretti, J. M. Blander, Cell-autonomous stress responses in innate immunity. *J Leukoc Biol* **101**, 77-86 (2017).
2. C. Franceschi, P. Garagnani, P. Parini, C. Giuliani, A. Santoro, Inflammaging: a new immune-metabolic viewpoint for age-related diseases. *Nat Rev Endocrinol* **14**, 576-590 (2018).
3. Y. Tong, S. Wang, Not All Stressors Are Equal: Mechanism of Stressors on RPE Cell Degeneration. *Front Cell Dev Biol* **8**, 591067 (2020).
4. D. A. Copland, S. Theodoropoulou, J. Liu, A. D. Dick, A Perspective of AMD Through the Eyes of Immunology. *Invest Ophthalmol Vis Sci* **59**, AMD83-AMD92 (2018).
5. J. T. Handa *et al.*, A systems biology approach towards understanding and treating non-neovascular age-related macular degeneration. *Nat Commun* **10**, 3347 (2019).
6. L. G. Fritsche *et al.*, A large genome-wide association study of age-related macular degeneration highlights contributions of rare and common variants. *Nat Genet* **48**, 134-143 (2016).
7. T. W. Winkler *et al.*, Genome-wide association meta-analysis for early age-related macular degeneration highlights novel loci and insights for advanced disease. *BMC Med Genomics* **13**, 120 (2020).
8. H. Khan *et al.*, Emerging Treatment Options for Geographic Atrophy (GA) Secondary to Age-Related Macular Degeneration. *Clin Ophthalmol* **17**, 321-327 (2023).
9. B. L. Yaspan *et al.*, Targeting factor D of the alternative complement pathway reduces geographic atrophy progression secondary to age-related macular degeneration. *Sci Transl Med* **9**, (2017).
10. B. Calippe *et al.*, Complement Factor H Inhibits CD47-Mediated Resolution of Inflammation. *Immunity* **46**, 261-272 (2017).
11. F. Beguier *et al.*, The 10q26 Risk Haplotype of Age-Related Macular Degeneration Aggravates Subretinal Inflammation by Impairing Monocyte Elimination. *Immunity* **53**, 429-441.e428 (2020).
12. C. B. Toomey, U. Kelly, D. R. Saban, C. Bowes Rickman, Regulation of age-related macular degeneration-like pathology by complement factor H. *Proc Natl Acad Sci U S A* **112**, E3040-3049 (2015).
13. S. Romero-Vazquez *et al.*, Interlink between Inflammation and Oxidative Stress in Age-Related Macular Degeneration: Role of Complement Factor H. *Biomedicines* **9**, (2021).

748 14. W. A. Tseng *et al.*, NLRP3 inflammasome activation in retinal pigment epithelial cells
749 by lysosomal destabilization: implications for age-related macular degeneration. *Invest*
750 *Ophthalmol Vis Sci* **54**, 110-120 (2013).

751 15. A. Klettner, J. Roider, Retinal Pigment Epithelium Expressed Toll-like Receptors and
752 Their Potential Role in Age-Related Macular Degeneration. *Int J Mol Sci* **22**, (2021).

753 16. V. Tarallo *et al.*, DICER1 loss and Alu RNA induce age-related macular degeneration via
754 the NLRP3 inflammasome and MyD88. *Cell* **149**, 847-859 (2012).

755 17. K. S. Lee, S. Lin, D. A. Copland, A. D. Dick, J. Liu, Cellular senescence in the aging
756 retina and developments of senotherapies for age-related macular degeneration. *J*
757 *Neuroinflammation* **18**, 32 (2021).

758 18. K. Mulfaul, M. Rhatigan, S. Doyle, Toll-Like Receptors and Age-Related Macular
759 Degeneration. *Adv Exp Med Biol* **1074**, 19-28 (2018).

760 19. L. Ma *et al.*, Association of toll-like receptor 3 polymorphism rs3775291 with age-
761 related macular degeneration: a systematic review and meta-analysis. *Sci Rep* **6**, 19718
762 (2016).

763 20. M. Hata *et al.*, Past history of obesity triggers persistent epigenetic changes in innate
764 immunity and exacerbates neuroinflammation. *Science* **379**, 45-62 (2023).

765 21. M. Kader *et al.*, MyD88-dependent inflammasome activation and autophagy inhibition
766 contributes to Ehrlichia-induced liver injury and toxic shock. *PLoS Pathog* **13**, e1006644
767 (2017).

768 22. S. Wang *et al.*, Deciphering primate retinal aging at single-cell resolution. *Protein Cell*
769 **12**, 889-898 (2021).

770 23. J. Liu *et al.*, Impairing autophagy in retinal pigment epithelium leads to inflammasome
771 activation and enhanced macrophage-mediated angiogenesis. *Sci Rep* **6**, 20639 (2016).

772 24. A. J. Clare, J. Liu, D. A. Copland, S. Theodoropoulou, A. D. Dick, Unravelling the
773 therapeutic potential of IL-33 for atrophic AMD. *Eye (Lond)*, (2021).

774 25. A. Jain, S. Kaczanowska, E. Davila, IL-1 Receptor-Associated Kinase Signaling and Its
775 Role in Inflammation, Cancer Progression, and Therapy Resistance. *Front Immunol* **5**,
776 553 (2014).

777 26. R. Gill, A. Tsung, T. Billiar, Linking oxidative stress to inflammation: Toll-like
778 receptors. *Free Radic Biol Med* **48**, 1121-1132 (2010).

779 27. J. Du *et al.*, The structure function of the death domain of human IRAK-M. *Cell*
780 *Commun Signal* **12**, 77 (2014).

781 28. H. Zhou *et al.*, IRAK-M mediates Toll-like receptor/IL-1R-induced NF κ B activation and
782 cytokine production. *EMBO J* **32**, 583-596 (2013).

783 29. L. L. Hubbard, B. B. Moore, IRAK-M regulation and function in host defense and
784 immune homeostasis. *Infect Dis Rep* **2**, (2010).

785 30. M. Hulsmans *et al.*, Interleukin-1 receptor-associated kinase-3 is a key inhibitor of
786 inflammation in obesity and metabolic syndrome. *PLoS One* **7**, e30414 (2012).

787 31. L. Balaci *et al.*, IRAK-M is involved in the pathogenesis of early-onset persistent asthma. *Am J Hum Genet* **80**, 1103-1114 (2007).

788 32. O. Zuk *et al.*, Searching for missing heritability: designing rare variant association
789 studies. *Proc Natl Acad Sci U S A* **111**, E455-464 (2014).

790 33. L. M. Scott *et al.*, Interleukin-33 regulates metabolic reprogramming of the retinal
791 pigment epithelium in response to immune stressors. *JCI Insight* **6**, (2021).

792 34. H. Xi *et al.*, IL-33 amplifies an innate immune response in the degenerating retina. *J Exp*
793 *Med* **213**, 189-207 (2016).

794 35. J. Augustine *et al.*, IL-33 deficiency causes persistent inflammation and severe
795 neurodegeneration in retinal detachment. *J Neuroinflammation* **16**, 251 (2019).

797 36. K. Kobayashi *et al.*, IRAK-M is a negative regulator of Toll-like receptor signaling. *Cell*
798 **110**, 191-202 (2002).

799 37. E. J. Kim *et al.*, Complete Transcriptome Profiling of Normal and Age-Related Macular
800 Degeneration Eye Tissues Reveals Dysregulation of Anti-Sense Transcription. *Sci Rep* **8**,
801 3040 (2018).

802 38. J. Tode *et al.*, Selective Retina Therapy Reduces Bruch's Membrane Thickness and
803 Retinal Pigment Epithelium Pathology in Age-Related Macular Degeneration Mouse
804 Models. *Transl Vis Sci Technol* **8**, 11 (2019).

805 39. D. E. Rothschild *et al.*, Enhanced Mucosal Defense and Reduced Tumor Burden in Mice
806 with the Compromised Negative Regulator IRAK-M. *EBioMedicine* **15**, 36-47 (2017).

807 40. S. M. Lange, M. I. Nelen, P. Cohen, Y. Kulathu, Dimeric Structure of the Pseudokinase
808 IRAK3 Suggests an Allosteric Mechanism for Negative Regulation. *Structure* **29**, 238-
809 251.e234 (2021).

810 41. P. Herrmann *et al.*, Cd59a deficiency in mice leads to preferential innate immune
811 activation in the retinal pigment epithelium-choroid with age. *Neurobiol Aging* **36**, 2637-
812 2648 (2015).

813 42. N. K. Wang *et al.*, Cellular origin of fundus autofluorescence in patients and mice with a
814 defective NR2E3 gene. *Br J Ophthalmol* **93**, 1234-1240 (2009).

815 43. Y. Ding, B. Aredo, X. Zhong, C. X. Zhao, R. L. Ufret-Vincenty, Increased susceptibility
816 to fundus camera-delivered light-induced retinal degeneration in mice deficient in
817 oxidative stress response proteins. *Exp Eye Res* **159**, 58-68 (2017).

818 44. C. Cingolani *et al.*, Retinal degeneration from oxidative damage. *Free Radic Biol Med*
819 **40**, 660-669 (2006).

820 45. P. Jin *et al.*, Activator protein 1 promotes the transcriptional activation of IRAK-M.
821 *Biomed Pharmacother* **83**, 1212-1219 (2016).

822 46. K. Lyroni *et al.*, Epigenetic and Transcriptional Regulation of IRAK-M Expression in
823 Macrophages. *J Immunol* **198**, 1297-1307 (2017).

824 47. M. A. Kanow *et al.*, Biochemical adaptations of the retina and retinal pigment epithelium
825 support a metabolic ecosystem in the vertebrate eye. *Elife* **6**, (2017).

826 48. S. E. Barker *et al.*, Subretinal delivery of adeno-associated virus serotype 2 results in
827 minimal immune responses that allow repeat vector administration in immunocompetent
828 mice. *J Gene Med* **11**, 486-497 (2009).

829 49. J. Guy *et al.*, Efficiency and safety of AAV-mediated gene delivery of the human ND4
830 complex I subunit in the mouse visual system. *Invest Ophthalmol Vis Sci* **50**, 4205-4214
831 (2009).

832 50. X. Qi, L. Sun, A. S. Lewin, W. W. Hauswirth, J. Guy, The mutant human ND4 subunit of
833 complex I induces optic neuropathy in the mouse. *Invest Ophthalmol Vis Sci* **48**, 1-10
834 (2007).

835 51. J. D. Ding *et al.*, Expression of human complement factor H prevents age-related macular
836 degeneration-like retina damage and kidney abnormalities in aged Cfh knockout mice.
837 *Am J Pathol* **185**, 29-42 (2015).

838 52. S. Russell *et al.*, Efficacy and safety of voretigene neparvovec (AAV2-hRPE65v2) in
839 patients with RPE65-mediated inherited retinal dystrophy: a randomised, controlled,
840 open-label, phase 3 trial. *Lancet* **390**, 849-860 (2017).

841 53. D. García-Ayuso, J. Di Pierdomenico, M. Vidal-Sanz, M. P. Villegas-Pérez, Retinal
842 Ganglion Cell Death as a Late Remodeling Effect of Photoreceptor Degeneration. *Int J
843 Mol Sci* **20**, (2019).

844 54. U. Greferath *et al.*, Inner retinal change in a novel rd1-FTL mouse model of retinal
845 degeneration. *Front Cell Neurosci* **9**, 293 (2015).

846 55. M. Zhang, W. Chen, W. Zhou, Y. Bai, J. Gao, Critical Role of IRAK-M in Regulating
847 Antigen-Induced Airway Inflammation. *Am J Respir Cell Mol Biol* **57**, 547-559 (2017).

848 56. Y. Ma, R. L. Haynes, R. L. Sidman, T. Vartanian, TLR8: an innate immune receptor in
849 brain, neurons and axons. *Cell Cycle* **6**, 2859-2868 (2007).

850 57. K. Kaarniranta *et al.*, Mechanisms of mitochondrial dysfunction and their impact on age-
851 related macular degeneration. *Prog Retin Eye Res* **79**, 100858 (2020).

852 58. M. V. Kumar, C. N. Nagineni, M. S. Chin, J. J. Hooks, B. Detrick, Innate immunity in
853 the retina: Toll-like receptor (TLR) signaling in human retinal pigment epithelial cells. *J
854 Neuroimmunol* **153**, 7-15 (2004).

855 59. B. Detrick, J. J. Hooks, Immune regulation in the retina. *Immunol Res* **47**, 153-161
856 (2010).

857 60. S. Sugita, M. Mandai, H. Kamao, M. Takahashi, Immunological aspects of RPE cell
858 transplantation. *Prog Retin Eye Res*, 100950 (2021).

859 61. I. Benhar, K. Reemst, V. Kalchenko, M. Schwartz, The retinal pigment epithelium as a
860 gateway for monocyte trafficking into the eye. *EMBO J* **35**, 1219-1235 (2016).

861 62. O. Levy *et al.*, Apolipoprotein E promotes subretinal mononuclear phagocyte survival
862 and chronic inflammation in age-related macular degeneration. *EMBO Mol Med* **7**, 211-
863 226 (2015).

864 63. W. Li *et al.*, Allicin attenuated hepatic ischemia/reperfusion injury in mice by regulating
865 PPAR γ -IRAK-M-TLR4 signal pathway. *Food Funct* **13**, 7361-7376 (2022).

866 64. C. Lyu *et al.*, IRAK-M Deficiency Exacerbates Ischemic Neurovascular Injuries in
867 Experimental Stroke Mice. *Front Cell Neurosci* **12**, 504 (2018).

868 65. A. Saxena *et al.*, The role of Interleukin Receptor Associated Kinase (IRAK)-M in
869 regulation of myofibroblast phenotype in vitro, and in an experimental model of non-
870 reperfused myocardial infarction. *J Mol Cell Cardiol* **89**, 223-231 (2015).

871 66. P. Mandrekar, S. Bala, D. Catalano, K. Kodys, G. Szabo, The opposite effects of acute
872 and chronic alcohol on lipopolysaccharide-induced inflammation are linked to IRAK-M
873 in human monocytes. *J Immunol* **183**, 1320-1327 (2009).

874 67. Y. Li *et al.*, Differential gene expression of interleukin-1 receptor associated kinase-1 and
875 interleukin-1 receptor associated kinase-M in peripheral blood mononuclear cells of
876 young and aged rats following preconditioning with endotoxin. *Shock* **31**, 55-63 (2009).

877 68. H. Domon, K. Tabeta, T. Nakajima, K. Yamazaki, Age-related alterations in gene
878 expression of gingival fibroblasts stimulated with *Porphyromonas gingivalis*. *J
879 Periodontal Res* **49**, 536-543 (2014).

880 69. A. Sheerin, K. S. Thompson, M. H. Goyns, Altered composition and DNA binding
881 activity of the AP-1 transcription factor during the ageing of human fibroblasts. *Mech
882 Ageing Dev* **122**, 1813-1824 (2001).

883 70. K. Riabowol, J. Schiff, M. Z. Gilman, Transcription factor AP-1 activity is required for
884 initiation of DNA synthesis and is lost during cellular aging. *Proc Natl Acad Sci U S A*
885 **89**, 157-161 (1992).

886 71. M. Helenius, M. Hänninen, S. K. Lehtinen, A. Salminen, Changes associated with aging
887 and replicative senescence in the regulation of transcription factor nuclear factor-kappa
888 B. *Biochem J* **318** (Pt 2), 603-608 (1996).

889 72. J. S. Tilstra, C. L. Clauson, L. J. Niedernhofer, P. D. Robbins, NF- κ B in Aging and
890 Disease. *Aging Dis* **2**, 449-465 (2011).

891 73. R. I. Martínez-Zamudio *et al.*, AP-1 imprints a reversible transcriptional programme of
892 senescent cells. *Nat Cell Biol* **22**, 842-855 (2020).

893 74. S. Leppä, D. Bohmann, Diverse functions of JNK signaling and c-Jun in stress response
894 and apoptosis. *Oncogene* **18**, 6158-6162 (1999).

895 75. B. J. Kim, D. J. Zack, The Role of c-Jun N-Terminal Kinase (JNK) in Retinal
896 Degeneration and Vision Loss. *Adv Exp Med Biol* **1074**, 351-357 (2018).
897 76. B. Chang, R. Hurd, J. Wang, P. Nishina, Survey of common eye diseases in laboratory
898 mouse strains. *Invest Ophthalmol Vis Sci* **54**, 4974-4981 (2013).
899 77. S. L. Klein, K. L. Flanagan, Sex differences in immune responses. *Nat Rev Immunol* **16**,
900 626-638 (2016).

901

902

903 **ACKNOWLEDGMENTS**

904 **Funding**

905 This work was funded by grants from Rosetrees Trust and Stoneygate Trust (Joint grant M418-
906 F1; ADD, JL and DAC), Underwood Trust (ADD), Macular Society (ADD, JL and DAC) and
907 Sight Research UK (grant SAC052; JL, ADD and DAC). The work was also supported by an
908 unrestricted grant to the Moran Eye Center from Research to Prevent Blindness, Inc. and
909 unrestricted funds from the Sharon Eccles Steele Center for Translation Medicine (GSH). We
910 thank the International AMD Genomics Consortium (IAMDGC), supported by the National Eye
911 Institute of the National Institutes of Health (grant 5R01EY022310). The work of IMH was
912 supported by the National Institutes of Health (grants RES516564 and RES511967).

913

914 **Author contributions**

915 Conceptualization: ADD, JL and YKC. Methodology: JL, ADD, YKC, GSH, IMH, MG, BR, UG,
916 MJR, ELF, RG, PJC, DAC and LBN. Investigation: JL, YKC, DAC, AJC, MG, BTR, GSH, LS,
917 ST, UG, KC, OHB, KO, JLBP, JW, LMR and YL. Visualization: ADD, JL and YKC. Supervision:
918 ADD, JL and YKC. Writing—original draft: JL, ADD and YKC. Writing—review & editing: all
919 authors.

920

921 **Competing interests**

922 ADD, JL and YKC are named inventors on an International Patent Application No:
923 PCT/EP2022/082518. ADD is consultant for Hubble Tx, Affibody, 4 DMT, Novartis, Roche,
924 UCB, Amilera, Janssen, and ActivBio. RG is consultant for Roche, Genentech, Apellis, Novartis,
925 and Bayer.

926

927 **Data and materials availability**

928 All data are available in the main text or the supplementary materials.